

Nonlinearly induced entanglement in dissipatively coupled optomechanical system

Wen-Quan Yang(杨文全), Xuan Leng(冷轩), Jiong Cheng(程泂), and Wen-Zhao Zhang(张闻钊)

Citation: Chin. Phys. B, 2024, 33 (**6**): 060313. DOI: 10.1088/1674-1056/ad3dd6
Journal homepage: http://cpb.iphy.ac.cn; http://iopscience.iop.org/cpb

What follows is a list of articles you may be interested in

Quantum circuit-based proxy blind signatures: A novel approach and experimental evaluation on the IBM quantum cloud platform

Xiaoping Lou(娄小平), Huiru Zan(咎慧茹), and Xuejiao Xu(徐雪娇)
Chin. Phys. B, 2024, 33 (**5**): 050307. DOI: 10.1088/1674-1056/ad22d5

Quantum correlations and entanglement in coupled optomechanical resonators with photon hopping via Gaussian interferometric power analysis

Y. Lahlou, B. Maroufi, and M. Daoud
Chin. Phys. B, 2024, 33 (**5**): 050303. DOI: 10.1088/1674-1056/ad2a6e

Complementary monogamy and polygamy properties among multipartite systems

Tao Li(李陶), Jing-Yi Zhou(周静怡), Qi Sun(孙琪), Zhi-Xiang Jin(靳志祥), Deng-Feng Liang(梁登峰), and Ting Luo(罗婷)
Chin. Phys. B, 2024, 33 (**3**): 030305. DOI: 10.1088/1674-1056/ad1748

Genuine entanglement under squeezed generalized amplitude damping channels with memory

Mazhar Ali
Chin. Phys. B, 2024, 33 (**2**): 020307. DOI: 10.1088/1674-1056/ace15f

Generation of hyperentangled photon pairs based on lithium niobate waveguide

Yang-He Chen(陈洋河), Zhen Jiang(姜震), and Guang-Qiang He(何广强)
Chin. Phys. B, 2023, 32 (**9**): 090306. DOI: 10.1088/1674-1056/acd5c4

Nonlinearly induced entanglement in dissipatively coupled optomechanical system

Wen-Quan Yang(杨文全), Xuan Leng(冷轩), Jiong Cheng(程泂), and Wen-Zhao Zhang(张闻钊)†

Department of Physics, Ningbo University, Ningbo 315211, *China*

(Received 9 March 2024; revised manuscript received 8 April 2024; accepted manuscript online 12 April 2024)

Nonlinearly induced steady-state photon–phonon entanglement of a dissipative coupled system is studied in the bistable regime. Quantum dynamical characteristics are analysed by solving the mean-field and fluctuation equations of the system. It is shown that dissipative coupling can induce bistable behaviour for the effective dissipation of the system. Under suitable parameters, one of the steady states significantly reduces the dissipative effect of the system. Consequently, a larger steady-state entanglement can be achieved compared to linear dynamics. Furthermore, the experimental feasibility of the parameters is analysed. Our results provide a new perspective for the implementation of steady-state optomechanical entanglement.

Keywords: entanglement, optomechanical system, dissipatively coupling

PACS: 03.67.Bg, 42.50.–p, 42.50.Wk **DOI:** 10.1088/1674-1056/ad3dd6

1. Introduction

Entanglement stands as a pivotal quantum resource[1–3] with extensive applications in quantum computation,[4–6] quantum information,[7–9] and so on. Various systems, including optical,[10] atomic,[11,12] and magnonic systems,[13,14] exhibit evident entanglement. Notably, the optomechanical system offers a versatile platform for studying photon–phonon entanglement,[15–17] thereby delving into fundamental theories and quantum information manipulation.[18,19] Optomechanical entanglement is investigated in both theoretical[20,21] and experimental[22–24] aspects. Recent attention has gravitated towards dissipative coupling optomechanical systems[25] in contrast to traditional dispersive coupling,[26] owing to their distinctive properties via optical dissipation modulation by mechanical displacement. Dissipative coupling was first proposed theoretically in Ref. [25] and confirmed experimentally in Ref. [27]. It has been observed in diverse systems, including Michelson–Sagnac interferometer with a movable membrane,[28] nanomechanical waveguide coupled with a microdisc resonator,[29] whispering-gallery mode coupled with a tapered fiber[30] and photonic crystal cavity.[31] Leveraging dissipative coupling, numerous physical phenomena have been investigated, encompassing electromagnetically induced transparency,[32,33] magnetic field induced nonreciprocity,[34] mechanical oscillator cooling,[25,35] and output light squeezing.[36,37]

Both dispersive and dissipative coupling, altering frequency and dissipation through mechanical oscillators, are fundamentally nonlinear in optomechanical systems.[26,38–40] These nonlinear effects have been extensively studied, including optical bistability,[40–42] optomechanically induced transparency,[38,43–46] quantum synchronization,[47,48] and photon blockade.[49–52] Notably, optomechanical coupling-induced nonlinearities offer advantages for entanglement.[24,43,53–55] Moreover, when combined with nonlinear effects, dissipative coupling holds promise in few-photon manipulation[56,57] by safeguarding quantum properties through optical bandwidth modulation. These studies provide a way to combine the advantages of nonlinear and dissipative coupling to protect and generate entanglement.

In this paper, we study the classical nonlinear effects of dissipative coupling system, and discuss quantum entanglement within the bistable region. We examine a hybrid coupled optomechanical system where dispersive and dissipation couplings coexist. The bistability of the mechanical oscillator displacement is determined by the dynamical analysis. Frequency and dissipation are simultaneously modulated the bistable mechanical oscillator in our system, which affects the quantum characteristics. Our results show that the dissipatively coupled optomechanical system with significant bistability can effectively enhance the driving strength. Specifically, with increasing dissipative coupling strength, both photon number and cavity dissipation experience a notable decrease in the bistability regime, and potentially reaching $\kappa_{\rm eff} \approx 0$ at the solvable boundary. More importantly, we find that nonlinearly induced entanglement is approximately 50 times higher than the linear case for experimentally achievable parameters. The paper is organized as follows. In Section 2, we introduce the system Hamiltonian and analyse the bistable region of a dissipatively coupled optomechanical system. In Section 3, we study the entanglement in the bistable region. Finally, we conclude and discuss the application prospects of our scheme in Section 4.

†Corresponding author. E-mail: zhangwenzhao@nbu.edu.cn

© 2024 Chinese Physical Society and IOP Publishing Ltd

2. Model and Hamiltonian

An optomechanical system in which the cavity frequency $\omega_{\rm c}$ (dispersive coupling) and the linewidth κ (dissipative coupling) are modulated by a mechanical oscillator is shown in Fig. 1. The Hamiltonian of the model is given by[28]

$$\begin{aligned}\hat{H}/\hbar =\ & \omega_{\rm c}(Q)\hat{c}^{\dagger}\hat{c}+\frac{1}{2}\omega_{\rm m}(\hat{Q}^2+\hat{P}^2)\\ & +{\rm i}\sqrt{\kappa(Q)}(\hat{c}^{\dagger}\hat{c}_{\rm in}\,{\rm e}^{-{\rm i}\omega_{\rm d}t}-\hat{c}\hat{c}_{\rm in}^{\dagger}\,{\rm e}^{{\rm i}\omega_{\rm d}t}),\end{aligned}\tag{1}$$

where $\omega_{\rm c}(Q)=\omega_{\rm c}+g_{\omega}\hat{Q}$ denotes the resonator displacement-modified optical frequency, and g_{ω} is the dispersive coupling rate (the commonly used optomechanical coupling rate). $\hat{c}$ is the bosonic operator of the cavity with frequency $\omega_{\rm c}$. $\hat{Q}=(\hat{b}+\hat{b}^{\dagger})/\sqrt{2}$ and $\hat{P}={\rm i}(\hat{b}^{\dagger}-\hat{b})/\sqrt{2}$ are the dimensionless displacement and momentum operators, respectively. $\hat{b}$ is the annihilation operator of the mechanical oscillator with frequency $\omega_{\rm m}$. $\hat{c}_{\rm in}=\varepsilon_{\rm d}+\hat{a}_{\rm in}$ denotes the input of the cavity, which contains a classical component ($\varepsilon_{\rm d}$) and a quantum component ($\hat{a}_{\rm in}$). $\varepsilon_{\rm d}=\sqrt{P_{\rm d}/(\hbar\omega_{\rm d})}$ is the amplitude of the laser driving with power $P_{\rm d}$ and frequency $\omega_{\rm d}$. $\hat{a}_{\rm in}$ is the input vacuum noise of the cavity with the correlation $\langle\hat{a}_{\rm in}(t)\hat{a}_{\rm in}^{\dagger}(t')\rangle=\delta(t-t')$. $\kappa(Q)=\kappa+g_{\kappa}\hat{Q}=\kappa(1+g_{\kappa}\hat{Q}/\kappa)$ is the resonator displacement-modified optical linewidth.[58] κ and g_{κ} denote uncoupled linewidth and dissipative coupling rate, respectively. In combination with the displacement-modified input–output relation, the dynamical equations of the system under frame rotation at the laser frequency in the Markovian regime are given by[28]

$$\dot{\hat{Q}} = \omega_{\rm m}\hat{P},\tag{2a}$$

$$\begin{aligned}\dot{\hat{P}} =\ & -\omega_{\rm m}\hat{Q}-g_{\omega}\hat{c}^{\dagger}\hat{c}-\frac{{\rm i}g_{\kappa}}{2\sqrt{\kappa(Q)}}(\hat{c}^{\dagger}\hat{c}_{\rm in}-\hat{c}\hat{c}_{\rm in}^{\dagger})\\ & -\gamma\hat{P}+\sqrt{\gamma}\hat{p}_{\rm in},\end{aligned}\tag{2b}$$

$$\dot{\hat{c}} = -\left[{\rm i}(\Delta_{\rm c}+g_{\omega}\hat{Q})+\frac{\kappa(Q)}{2}\right]\hat{c}+\sqrt{\kappa(Q)}\hat{c}_{\rm in},\tag{2c}$$

where $\Delta_{\rm c}=\omega_{\rm c}-\omega_{\rm d}$ is the detuning between the cavity and the input laser. γ is the mechanical damping rate and $\hat{p}_{\rm in}$ is the mechanical input noise operator satisfying $\langle\hat{p}_{\rm in}^{\dagger}(\omega)\hat{p}_{\rm in}(\omega')\rangle=\delta(\omega-\omega')n_{\rm th}$, where $n_{\rm th}=[\exp(\hbar\omega_{\rm m}/k_{\rm B}T)-1]^{-1}$ describes the thermal phonon number with temperature T. In the above Langevin Eq. (2), the commutation relation $[\hat{P},\sqrt{\kappa(Q)}]=-\frac{{\rm i}g_{\kappa}}{2\sqrt{\kappa(Q)}}$ is obtained by utilizing the expansion of the series $\sqrt{\kappa(Q)}=\sqrt{\kappa}\sum_{n=0}^{\infty}\frac{(1/2)(1/2-1)\cdots(1/2-n+1)}{n!}(\frac{g_{\kappa}\hat{Q}}{\kappa})^n$ and the commutation formula $[\hat{P},\hat{Q}^n]=-{\rm i}n\hat{Q}^{n-1}$. Under the strong driving and weak coupling condition, we can decompose the above dynamical equations into a nonlinear classical part and a linear quantum part. The corresponding operator can be divided as $\hat{Q}=\bar{Q}+\hat{q}$, $\hat{P}=\bar{P}+\hat{p}$, $\hat{c}=\bar{c}+\hat{a}$, in which $\bar{O}\equiv\langle\hat{O}\rangle$. A series expansion of $\sqrt{\kappa(Q)}=\sqrt{\kappa}\sqrt{1+g_{\kappa}\bar{Q}/\kappa+g_{\kappa}\hat{q}/\kappa}$ yields $\sqrt{\kappa}(\sqrt{1+g_{\kappa}\bar{Q}/\kappa}+\frac{g_{\kappa}\hat{q}/\kappa}{2\sqrt{1+g_{\kappa}\bar{Q}/\kappa}})+O[g_{\kappa}\hat{q}/\kappa]^2$. Under the condition $g_{\kappa}\hat{q}/\kappa\ll 1$, we can make use of the first-order approximate $\sqrt{\kappa(Q)}\approx\sqrt{\kappa}(\sqrt{1+g_{\kappa}\bar{Q}/\kappa}+\frac{g_{\kappa}\hat{q}/\kappa}{2\sqrt{1+g_{\kappa}\bar{Q}/\kappa}})$. The nonlinear classical dynamical equations are

$$\begin{aligned}\dot{\bar{Q}} =\ & \omega_{\rm m}\bar{P},\\ \dot{\bar{P}} =\ & -\omega_{\rm m}\bar{Q}-g_{\omega}\bar{c}^{*}\bar{c}-\frac{{\rm i}g_{\kappa}\varepsilon_{\rm d}}{2\sqrt{\kappa+g_{\kappa}\bar{Q}}}(\bar{c}^{*}-\bar{c})-\gamma\bar{P},\\ \dot{\bar{c}} =\ & -\left[{\rm i}(\Delta_{\rm c}+g_{\omega}\bar{Q})+\frac{1}{2}(\kappa+g_{\kappa}\bar{Q})\right]\bar{c}\\ & +\sqrt{\kappa+g_{\kappa}\bar{Q}}\varepsilon_{\rm d}.\end{aligned}\tag{3}$$

For exploring the long-time dynamical behavior or detection of quantum systems, we can safely use the classical steady-state solutions to modify the parameters in quantum dynamics. Under this premise, Eq. (3) can be written as

$$\begin{aligned}0 =\ & -\omega_{\rm m}\bar{Q}-g_{\omega}\bar{c}^{*}\bar{c}-\frac{{\rm i}g_{\kappa}\varepsilon_{\rm d}}{2\sqrt{\kappa+g_{\kappa}\bar{Q}}}(\bar{c}^{*}-\bar{c}),\\ 0 =\ & -\left[{\rm i}(\Delta_{\rm c}+g_{\omega}\bar{Q})+\frac{1}{2}(\kappa+g_{\kappa}\bar{Q})\right]\bar{c}\\ & +\sqrt{\kappa+g_{\kappa}\bar{Q}}\varepsilon_{\rm d}.\end{aligned}\tag{4}$$

It is evident that the classical part of the system exhibits typical characteristics of nonlinear dynamics. The mean-field-modified linearized quantum dynamical equations are

$$\begin{aligned}\dot{\hat{q}} =\ & \omega_{\rm m}\hat{p},\\ \dot{\hat{p}} =\ & -\omega_{\rm m}\hat{q}-(G_{\omega}^{*}\hat{a}+G_{\omega}\hat{a}^{\dagger})-\gamma\hat{p}+\sqrt{\gamma}\hat{p}_{\rm in}\\ & -\frac{\rm i}{\sqrt{\kappa_{\rm eff}}}\left[(G_{\kappa}^{*}\hat{a}_{\rm in}-G_{\kappa}\hat{a}_{\rm in}^{\dagger})+\frac{g_{\kappa}\varepsilon_{\rm d}}{2}(\hat{a}^{\dagger}-\hat{a})\right],\\ \dot{\hat{a}} =\ & -({\rm i}\omega_{\rm eff}+\kappa_{\rm eff})\hat{a}-(G_{\kappa}+{\rm i}G_{\omega})\hat{q}\\ & +\sqrt{\kappa_{\rm eff}}\hat{a}_{\rm in}+\frac{g_{\kappa}\varepsilon_{\rm d}}{2\sqrt{\kappa_{\rm eff}}}\hat{q},\end{aligned}\tag{5}$$

where $G_{\omega}=\bar{c}g_{\omega}$ and $G_{\kappa}=\bar{c}g_{\kappa}/2$ denote the mean-field-enhanced dispersive and dissipative coupling, respectively. $\omega_{\rm eff}=\Delta_{\rm c}+g_{\omega}\bar{Q}$ and $\kappa_{\rm eff}=\kappa+g_{\kappa}\bar{Q}$ denote the mean-displacement-modified frequency and dissipation, respectively. It is evident that the classical mean value impacts the behavior of quantum dynamics through the parameters. For conventional optomechanical systems, the displacement of the movable mirror by optical force action reduces the optical frequency through the cavity length. According to the expression of $\omega_{\rm eff}$, we can obtain that $\bar{Q}$ is negative. In weak driving and linear conditions, the value of $\bar{Q}$ is generally small and is usually ignored. However, under nonlinear conditions, $\bar{Q}$ can be significant and has a non-negligible decrease to $\omega_{\rm eff}$ and $\kappa_{\rm eff}$. This nonlinear dynamics affects the equations of the quantum part through effective frequency, effective dissipation, and average photon number ($n_{\rm s}=\bar{c}^{*}\bar{c}$), thus exhibiting different quantum characteristics of the system.

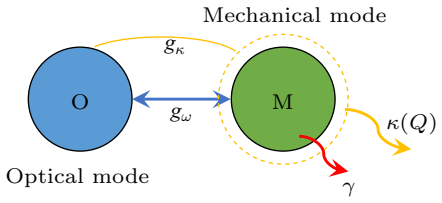


Fig. 1. Schematic structure of the dissipative coupled system, where the dissipation of the optical mode O is modulated by the mechanical mode M.

As shown in Fig. 2, classical nonlinear behavior is illustrated. The grey area in the figure represents the unsolvable parameter region, where the roots are mathematically legitimate but do not correspond to any physical meaning (the solutions in this region do not satisfy the law of conservation of energy). The dotted-lines indicate unstable branches of the system,[42,59] which represent the transition state between the two steady states. It is similar to the peak point of the potential field, although the solution at this point exists, all the energy around it is lower, thus with a slight perturbation, the state of the system will fall to one of the two steady states. As the driving strength or coupling rate is increased from small values, the system is initially at the first stable branch labelled as I and represented by the solid-line in the figure. When the parameters approach the end of the I branch, a small increase will cause a switch of $\{n_s, \kappa_{\rm eff}, \omega_{\rm eff}\}$ to the second stable branch II with dashed-line. Conversely, when the system is on the II branch, the parameters approach the beginning of the second stable branch. If the parameters are decreased even further, the system switches back to the I stable branch. As shown in Fig. 2(a), the enhancement of the dissipative coupling g_κ decreases the steady-state photon number in the cavity. When the dissipative coupling coefficient reaches a certain value such as $g_\kappa = 5\times10^{-5}\omega_{\rm m}$, n_s gradually tends to 0 with the increase of the driving strength. A similar conclusion is demonstrated in Fig. 2(b). As the driving strength increases, the effective dissipation gradually tends to 0 with $g_\kappa = 5\times10^{-5}\omega_{\rm m}$. This is a phenomenon distinct from the bistable behavior of conventional optomechanical systems and is an additional effect introduced by dissipative coupling. According to the expression for effective dissipation $\kappa_{\rm eff} = \kappa + g_\kappa\bar{Q}$, the modulation is only available when $g_\kappa \neq 0$ (see red line in the figure). Furthermore, it is known from the Hamiltonian that the driving is introduced through external input, which means when the effective dissipation is 0, there is no effective input exists. This explains the phenomenon in Fig. 2(a) where the photon number drops to 0 when dissipative coupling is present. As shown in Fig. 2(c), the effective detuning switches from beam-splitter type (BS-type) coupling to parametric down-conversion type (PDC-type) coupling under the modulation of the driving, regardless of the presence of dissipative coupling. This means we can modulate quantum effects, such as entanglement, by controlling classical driving.[60] For g_ω, the key parameter for inducing nonlinearity, there is a similar effect to that of the driving, where the system exhibits bistability as g_ω increases, and the corresponding results are shown in Figs. 2(d)–2(f). Due to the introduction of dissipative coupling, there is an effective dissipation $\kappa_{\rm eff} \approx 0$ on the beginning of the second stable branch ($\kappa_{\rm eff} = 0$ is a singularity, which we mark with a black dot in the figure also classified as an unsolvable region). It is worth noting that in Fig. 2(d), the unstable and upper solutions are misaligned in the presence of a dissipative coupling g_κ. In the figure, the unstable solution shifts up while the upper solution shifts down. The reason for this phenomenon is as we analyzed above, the unstable solution does not satisfy the law of energy conservation. When dissipation decreases, the effective input energy of the driving also decreases, and naturally the upper stable branch decreases, whereas the unstable solution does not satisfy this law.

According to Eq. (5), we can obtain the effective Hamiltonian of the quantum component modified by the classical dynamics,

$$\hat{H}_{\rm eff}/\hbar = \left(\omega_{\rm eff} - \frac{\rm i}{2}\kappa_{\rm eff}\right)\hat{a}^\dagger\hat{a} + \frac{\omega_{\rm m}}{2}(\hat{p}^2+\hat{q}^2) + \left(G^*_{\rm eff}\hat{a} + G_{\rm eff}\hat{a}^\dagger\right)\hat{q}, \tag{6}$$

where $G_{\rm eff} = G_\omega - {\rm i}G_\kappa + {\rm i}\frac{g_\kappa\varepsilon_{\rm d}}{2\sqrt{\kappa_{\rm eff}}}$ and $G^*_{\rm eff} = G^*_\omega - {\rm i}G^*_\kappa - {\rm i}\frac{g_\kappa\varepsilon_{\rm d}}{2\sqrt{\kappa_{\rm eff}}}$ denote the linearized total coupling coefficient between the optical and mechanical modes. Note that the effective Hamiltonian contains the dissipative term of the optical mode, which is due to the fact that the dissipative coupling leads to a modification of the input–output relation of the optical cavity.[58] Since the dissipative coupling originates from the correction of the oscillator to the optical environment, which is non-Hermitian in the Markov regime, thus the term $G_{\rm eff}$ in the Hamiltonian containing the dissipative coupling is also non-Hermitian. The $G_{\rm eff}$ and $G^*_{\rm eff}$ inversely written from the dynamical equations are also not conjugate.

For bipartite Gaussian states, entanglement is discussed in dispersive coupled optomechanical systems within the bistable region.[42] The introduction of dissipative coupling in our discussion demonstrates distinct differences and advantages over purely dispersive coupled systems. Thus, it is necessary to discuss the entanglement characteristics in dissipative coupled systems. In terms of the covariance matrix formalism the criterion is called logarithmic negativity, which is defined as[61,62] $E_{\rm n} = \max[0, -\ln(2\eta^-)]$, where η^- is the smallest symplectic eigenvalue of the partially transposed covariance matrix given by $\eta^- = (1/\sqrt{2}[\Sigma(\boldsymbol{V}) - \sqrt{\Sigma(\boldsymbol{V})^2 - 4\det\boldsymbol{V}}]^{1/2})$ and $\Sigma(\boldsymbol{V}) = \det(\boldsymbol{V}_{\rm A}) + \det(\boldsymbol{V}_{\rm B}) - 2\det(\boldsymbol{V}_{\rm C})$. Here, $\boldsymbol{V}_{\rm A}$, $\boldsymbol{V}_{\rm B}$, and

$\boldsymbol{V}_{\rm C}$ are 2×2 matrices obtained via the covariance matrix[63]

$$\boldsymbol{V}=\begin{pmatrix}\boldsymbol{V}_{\rm A} & \boldsymbol{V}_{\rm C}\\ \boldsymbol{V}_{\rm C}^{\rm T} & \boldsymbol{V}_{\rm B}\end{pmatrix}. \tag{7}$$

The elements of the covariance matrix are defined as $V_{ij}=\langle\hat{u}_i\hat{u}_j+\hat{u}_j\hat{u}_i\rangle/2$, in which $\hat{\boldsymbol{u}}=(\hat{X},\hat{Y},\hat{q},\hat{p})^{\rm T}$. The optical quadrature operators are defined as $\hat{X}=(\hat{a}+\hat{a}^{\dagger})/\sqrt{2}$ and $\hat{Y}={\rm i}(\hat{a}^{\dagger}-\hat{a})/\sqrt{2}$. The equation of motion for the covariance matrix is given by[64]

$$\dot{\boldsymbol{V}}(t)=\boldsymbol{A}(t)\boldsymbol{V}(t)+\boldsymbol{V}(t)\boldsymbol{A}^{\rm T}(t)+\boldsymbol{D}, \tag{8}$$

where the input noise matrix $\boldsymbol{D}={\rm diag}(\kappa_{\rm eff}/2,\kappa_{\rm eff}/2,0,\gamma n'_{\rm th})$ with $n'_{\rm th}=n_{\rm th}+|G_\kappa|^2/(\kappa_{\rm eff}\gamma)$ being the effective thermal noise. With the help of the effective Hamiltonian, the system coefficient matrix is given by

$$\boldsymbol{A}=\begin{pmatrix}-\frac{\kappa_{\rm eff}}{2} & \omega_{\rm eff} & \frac{G^*_{\rm eff}-G_{\rm eff}}{\sqrt{2}} & 0\\ -\omega_{\rm eff} & -\frac{\kappa_{\rm eff}}{2} & \frac{{\rm i}(G^*_{\rm eff}+G_{\rm eff})}{\sqrt{2}} & 0\\ 0 & 0 & 0 & \omega_{\rm m}\\ \frac{-(G^*_{\rm eff}+G_{\rm eff})}{\sqrt{2}} & \frac{{\rm i}(G_{\rm eff}-G^*_{\rm eff})}{\sqrt{2}} & -\omega_{\rm m} & -\gamma\end{pmatrix}. \tag{9}$$

Figure 3 shows the steady-state logarithmic negativity as a function of driving strength $\varepsilon_{\rm d}$. To visualize the behavior of entanglement in the bistable regime, we select the BS-type sideband (such sideband is unentangled in the linear case for the system), i.e., $\Delta_{\rm c}=\omega_{\rm m}$. As shown in the figure, as the driving increases, nonlinear effects emerge and the effective detuning gradually shifts from the BS-type sideband to the PDC-type sideband where entanglement can be generated. In the first stable branch of the system, tiny entanglement appears due to small changes in effective detuning, marked with the yellow area I in the figure. Dissipative coupling in this region can enhance entanglement. In the second stable branch, large entanglement emerges. In this region, the effective detuning is close to $-\omega_{\rm m}$, and entanglement reaches a maximum when the system is driven to the PDC-type sideband. Dissipative coupling is significant for entanglement in this region, marked with grey area. The entanglement is much larger with $g_\kappa=5\times10^{-5}\omega_{\rm m}$ than with $g_\kappa=0$ and $g_\kappa=10^{-5}\omega_{\rm m}$. This is because the effective dissipation tends to 0 in the $g_\kappa=5\times10^{-5}\omega_{\rm m}$ case (see Fig. 2(b)), thus the large steady state entanglement is highlighted. It is worth noting that although the mean-field of the system is nonlinear, the quantum part remains linear, ensuring Gaussianity in the computational process and the availability of entanglement criteria. For the unstable solution in Fig. 2 (dotted-line), since this part of the solution is not energy-conserving, the decay brought by the dissipative coupling in $G_{\rm eff}$ is much stronger than the energy introduced by the driving. As a result, the non-diagonal elements rapidly decay to 0, and no entanglement will be induced. Hence, no special treatment is needed to deal with this part in Fig. 3.

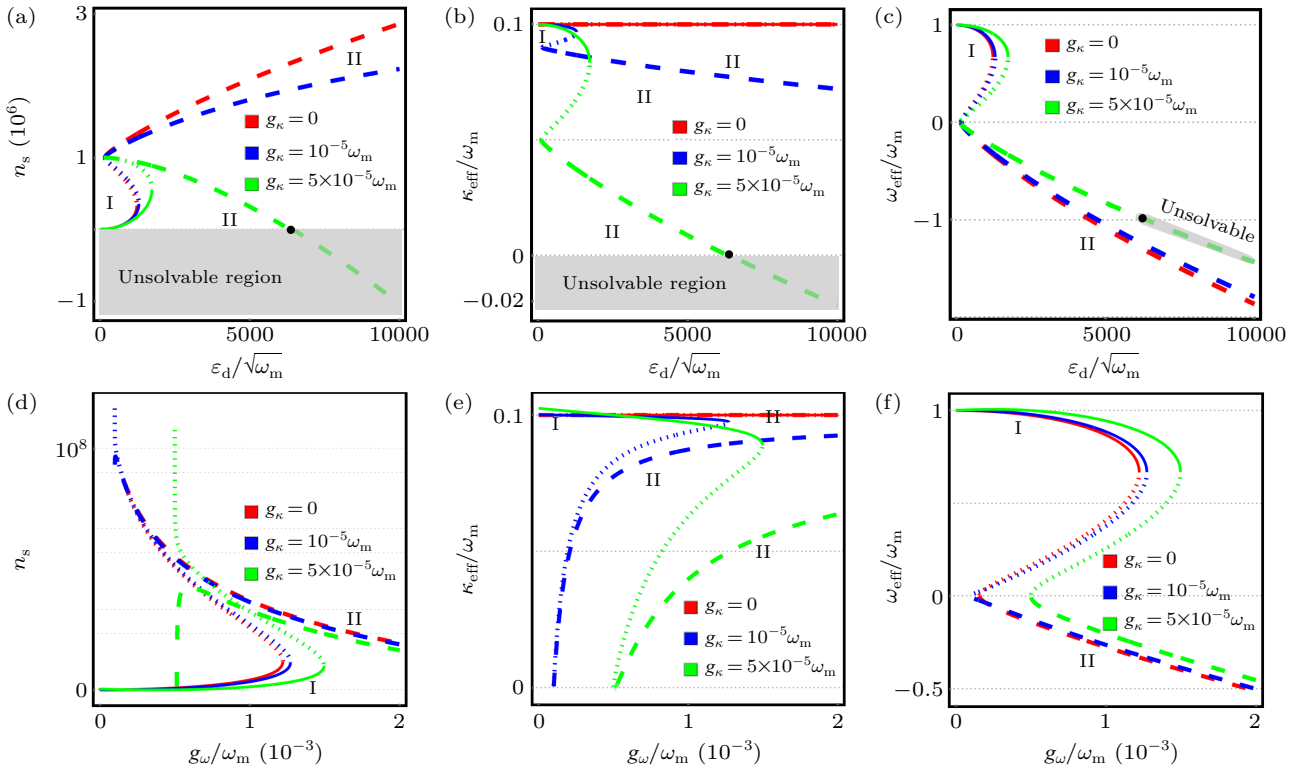


Fig. 2. Bistability of the intracavity photon number, effective dissipation and effective frequency with respect to (a)–(c) input power and (d)–(e) coupling rate g_ω. The other parameters are $\Delta_{\rm c}=\omega_{\rm m}$, $g_\omega/\omega_{\rm m}=10^{-3}$, $\kappa/\omega_{\rm m}=0.1$, $\varepsilon_{\rm d}/\omega_{\rm m}=10^3$, $\gamma/\omega=10^{-5}$, $n_{\rm th}=100$.

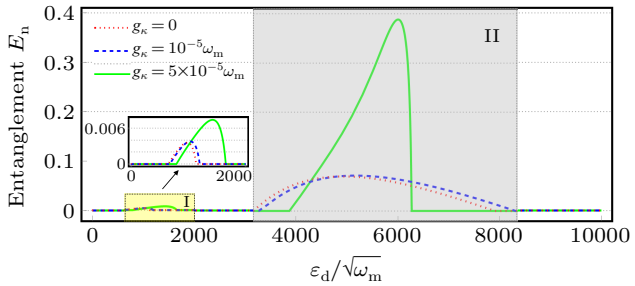


Fig. 3. Steady-state entanglement in the bistable regime with different g_κ. The yellow region indicates entanglement induced by the I branch and the grey region indicates entanglement induced by the II branch. The other parameters are the same as in Fig. 2.

3. Discussion and conclusions

Dissipative coupling has been experimentally realized in membrane optomechanical systems[27,65] and crystal optomechanical systems.[31,66] Among these, the membrane optomechanical system offers adjustable coupling coefficients g_ω and g_κ, but the coupling strength is weak,[27,28,65] whereas the crystal optomechanical system provides stronger coupling, albeit with challenging adjustments of g_ω and g_κ.[31,66] In our discussion, no specific requirements are imposed on the system parameters. The key to achieving bistability lies in the coupling coefficient g_ω and the driving strength ε_d. If the g_ω of the system is small, a robust laser driving becomes necessary, and the commonly used driving strengths in experiments are on the order of mW. The corresponding $\varepsilon_d/\omega_m \sim 10^8$ with 1550 nm optical laser and 5.5 GHz mechanical resonator,[66] which far exceeds the driving strengths depicted in our figures. Thus, our discussion is within the scope of an experiment.

We have investigated the entanglement behavior in the dissipative coupled optomechanical system in the bistable regime. Dissipative coupling allows the system to achieve large steady-state entanglement by eliminating the effective dissipation, which is different from the nonlinearly induced weak entanglement in purely dispersion-coupled systems. Dissipatively coupled systems lead to rich physics, both in terms of frequency modulation by classical nonlinearities and, more importantly, the induction of dissipation modulation, which makes it possible to protect or highlight the quantum behavior of the system through dissipative coupling. Our study provides a new perspective for the protection of the quantum effect by dissipative coupling.

Acknowledgments

We thank Chen-Jie Zhang for the instructive discussions. Project supported by the National Natural Science Foundation of China (Grant No. 12074206) and the Natural Science Foundation of Zhejiang Province of China (Grant No. LY22A040005). Xuan Leng is supported by the National Natural Science Foundation of China (Grant No. 22103043).

References

[1] Horodecki R, Horodecki P, Horodecki M and Horodecki K 2009 *Rev. Mod. Phys.* **81** 865
[2] Pan J W, Chen Z B, Lu C Y, Weinfurter H, Zeilinger A and Żukowski M 2012 *Rev. Mod. Phys.* **84** 777
[3] Chitambar E and Gour G 2019 *Rev. Mod. Phys.* **91** 025001
[4] Kok P, Munro W J, Nemoto K, Ralph T C, Dowling J P and Milburn G J 2007 *Rev. Mod. Phys.* **79** 135
[5] Galindo A and Martín-Delgado M A 2002 *Rev. Mod. Phys.* **74** 347
[6] Maier T, Jarrell M, Pruschke T and Hettler M H 2005 *Rev. Mod. Phys.* **77** 1027
[7] Weedbrook C, Pirandola S, García-Patrón R, Cerf N J, Ralph T C, Shapiro J H and Lloyd S 2012 *Rev. Mod. Phys.* **84** 621
[8] Clausen C, Usmani I, Bussières F, Sangouard N, Afzelius M, de Riedmatten H and Gisin N 2011 *Nature* **469** 508
[9] Zhao J, Li W and Gu Y 2013 *Europhys. Lett.* **104** 10005
[10] Wu S X, Bai C H, Li G, Yu C S and Zhang T 2024 *Opt. Express* **32** 260
[11] Yin X L and Liao J Q 2023 *Phys. Rev. A* **108** 023728
[12] Zhou L, Xiong H and Zubairy M S 2006 *Phys. Rev. A* **74** 022321
[13] Yu M, Shen H and Li J 2020 *Phys. Rev. Lett.* **124** 213604
[14] Li J, Zhu S Y and Agarwal G S 2018 *Phys. Rev. Lett.* **121** 203601
[15] Chen Z X, Lin Q, He B and Lin Z Y 2017 *Opt. Express* **25** 17237
[16] Sinha K, Lin S Y and Hu B L 2015 *Phys. Rev. A* **92** 023852
[17] Zhou L, Han Y, Jing J and Zhang W 2011 *Phys. Rev. A* **83** 052117
[18] Beckey J L, Ma Y, Boyer V and Miao H 2019 *Phys. Rev. D* **100** 083011
[19] Wang Y D, Chesi S and Clerk A A 2015 *Phys. Rev. A* **91** 013807
[20] Wang Y D and Clerk A A 2013 *Phys. Rev. Lett.* **110** 253601
[21] You X and Li Y 2019 *Phys. Rev. A* **100** 053842
[22] Xia Y, Agrawal A R, Pluchar C M, Brady A J, Liu Z, Zhuang Q, Wilson D J and Zhang Z 2023 *Nat. Photonics* **17** 470
[23] Fiaschi N, Hensen B, Wallucks A, Benevides R, Li J, Alegre T P M and Gröblacher S 2021 *Nat. Photonics* **15** 817
[24] Riedinger R, Wallucks A, Marinković I, Löschnauer C, Aspelmeyer M, Hong S and Gröblacher S 2018 *Nature* **556** 473
[25] Elste F, Girvin S M and Clerk A A 2009 *Phys. Rev. Lett.* **102** 207209
[26] Aspelmeyer M, Kippenberg T J and Marquardt F 2014 *Rev. Mod. Phys.* **86** 1391
[27] Sawadsky A, Kaufer H, Nia R M, Tarabrin S P, Khalili F Y, Hammerer K and Schnabel R 2015 *Phys. Rev. Lett.* **114** 043601
[28] Xuereb A, Schnabel R and Hammerer K 2011 *Phys. Rev. Lett.* **107** 213604
[29] Li M, Pernice W H P and Tang H X 2009 *Phys. Rev. Lett.* **103** 223901
[30] Meng J W, Tang S J, Sun J, Shen K, Li C, Gong Q and Xiao Y F 2022 *Phys. Rev. Lett.* **129** 073901
[31] Wu M, Hryciw A C, Healey C, Lake D P, Jayakumar H, Freeman M R, Davis J P and Barclay P E 2014 *Phys. Rev. X* **4** 021052
[32] Weiss T, Bruder C and Nunnenkamp A 2013 *New J. Phys.* **15** 045017
[33] Huang S, Deng L and Chen A 2023 *Phys. Rev. A* **107** 013524
[34] Biehs S A and Agarwal G S 2023 *Phys. Rev. B* **108** 035423
[35] Liu Y, Liu Y, Hu C S, Jiang Y K, Wu H and Li Y 2023 *Phys. Rev. A* **108** 023503
[36] Tagantsev A K, Sokolov I V and Polzik E S 2018 *Phys. Rev. A* **97** 063820
[37] Qu K and Agarwal G S 2015 *Phys. Rev. A* **91** 063815
[38] Safavi-Naeini A H, Alegre T P M, Chan J, Eichenfield M, Winger M, Lin Q, Hill J T, Chang D E and Painter O 2011 *Nature* **472** 69
[39] Eichenfield M, Chan J, Camacho R M, Vahala K J and Painter O 2009 *Nature* **462** 78
[40] Sete E A and Eleuch H 2012 *Phys. Rev. A* **85** 043824
[41] Marquardt F, Harris J G E and Girvin S M 2006 *Phys. Rev. Lett.* **96** 103901
[42] Ghobadi R, Bahrampour A R and Simon C 2011 *Phys. Rev. A* **84** 033846
[43] Weis S, Rivière R, Deléglise S, Gavartin E, Arcizet O, Schliesser A and Kippenberg T J 2010 *Science* **330** 1520
[44] Agarwal G S and Huang S 2010 *Phys. Rev. A* **81** 041803
[45] Wu Z, Luo R H, Zhang J Q, Wang Y H, Yang W and Feng M 2017 *Phys. Rev. A* **96** 033832
[46] Ma P C, Zhang J Q, Xiao Y, Feng M and Zhang Z M 2014 *Phys. Rev. A* **90** 043825
[47] Li W, Li C and Song H 2017 *Phys. Rev. E* **95** 022204
[48] Cheng J, Li W and Li J 2023 *Phys. Rev. Res.* **5** 043197

[49] Rabl P 2011 *Phys. Rev. Lett.* **107** 063601
[50] Huang R, Miranowicz A, Liao J Q, Nori F and Jing H 2018 *Phys. Rev. Lett.* **121** 153601
[51] Liao J Q and Nori F 2013 *Phys. Rev. A* **88** 023853
[52] Zhang W Z, Cheng J, Liu J Y and Zhou L 2015 *Phys. Rev. A* **91** 063836
[53] Wang G, Huang L, Lai Y C and Grebogi C 2014 *Phys. Rev. Lett.* **112** 110406
[54] Vitali D, Gigan S, Ferreira A, Böhm H R, Tombesi P, Guerreiro A, Vedral V, Zeilinger A and Aspelmeyer M 2007 *Phys. Rev. Lett.* **98** 030405
[55] Kotler S, Peterson G A, Shojaee E, Lecocq F, Cicak K, Kwiatkowski A, Geller S, Glancy S, Knill E, Simmonds R W, Aumentado J and Teufel J D 2021 *Science* **372** 622
[56] Gao Y P and Wang C 2021 *Opt. Express* **29** 25161
[57] Kilda D and Nunnenkamp A 2016 *J. Opt.* **18** 014007
[58] Primo A G, Carvalho N C, Kersul C M, Frateschi N C, Wiederhecker G S and Alegre T P M 2020 *Phys. Rev. Lett.* **125** 233601
[59] Boulier T, Bamba M, Amo A, Adrados C, Lemaitre A, Galopin E, Sagnes I, Bloch J, Ciuti C, Giacobino E and Bramati A 2014 *Nat. Commun.* **5** 3260
[60] Zhang J, Mu Q X and Zhang W Z 2018 *Chin. Phys. B* **27** 040304
[61] Adesso G, Serafini A and Illuminati F 2004 *Phys. Rev. A* **70** 022318
[62] Plenio M B 2005 *Phys. Rev. Lett.* **95** 090503
[63] Vitali D, Tombesi P, Woolley M J, Doherty A C and Milburn G J 2007 *Phys. Rev. A* **76** 042336
[64] Mari A and Eisert J 2009 *Phys. Rev. Lett.* **103** 213603
[65] Meyer H M, Breyer M and Köhl M 2016 *Appl. Phys. B* **122** 290
[66] Primo A G, Pinho P V, Benevides R, Gröblacher S, Wiederhecker G S and Alegre T P M 2023 *Nat. Commun.* **14** 5793